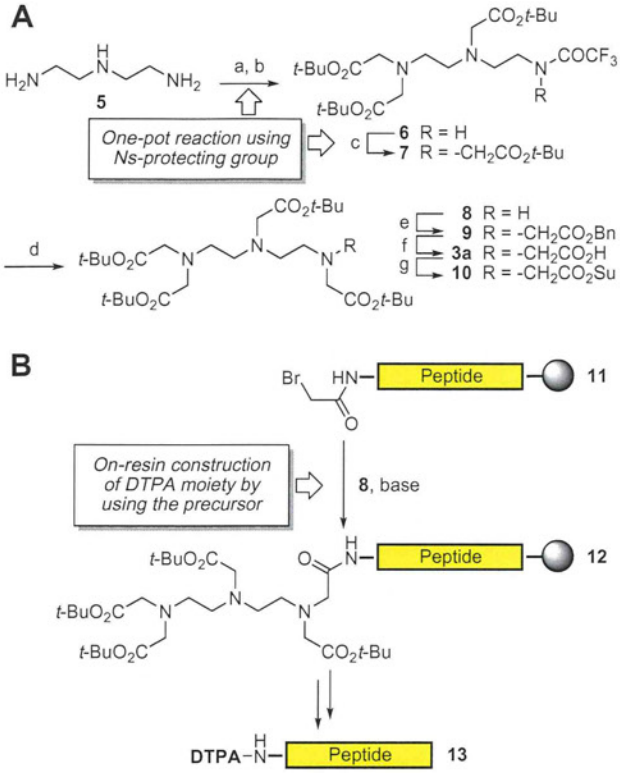

Scheme 1. (A) Synthetic scheme for the DTPA-conjugation reagent **10** prepared in our previous study; (B) synthetic plan for the DTPA-conjugated peptides in this study. Reagents: (a) CF_3CO_2Et; (b) $BrCH_2CO_2t$-Bu, $(i\text{-}Pr)_2NEt$; (c) $BrCH_2CO_2t$-Bu, NaH; (d) NH_2NH_2, *t*-BuOH; (e) $BrCH_2CO_2Bn$, $(i\text{-}Pr)_2NEt$; (f) H_2, Pd/C; (g) DCC, HOSu.

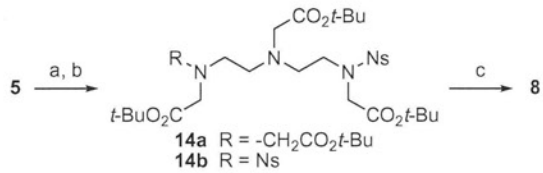

Scheme 2. Synthesis of DTPA precursor **8** via a global N-alkylation process using a Ns-protecting group. Reagents: (a) NsCl; (b) $BrCH_2CO_2t$-Bu, K_2CO_3; (c) $HSCH_2CO_2H$, LiOH.

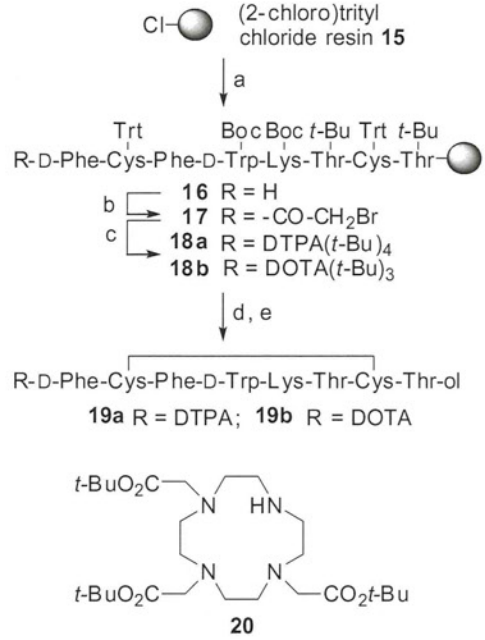

Scheme 3. Synthesis of DTPA- and DOTA-conjugated D-Phe-octreotides. Reagents: (a) Fmoc-based peptide synthesis; (b) $BrCH_2CO_2H$, DIC; (c) **8** for **18a**, or **20** for **18b**, $(i\text{-}Pr)_2NEt$ (d) TFA/H_2O/1,2-ethanedithiol (EDT) (95:2.5:2.5) for **19a**, 1 M TMSBr, thioanisole/TFA, 1,2-ethanedithiol, *m*-cresol for **19b**; (e) NH_4OH (air oxidation).

26b,c, a Boc group was employed. This group can be cleaved by the standard TFA-based treatment in Fmoc chemistry (Scheme 4). After the construction of the protected peptide resin, the orthogonal Mtt group at the labeling position was cleaved off using 1,1,1,3,3,3-hexafluoropropan-2-ol (HFIP). The resulting ε-amino group was successively modified with bromoacetic acid followed by the reagent **8** to provide the fully protected DTPA–peptide resin **25**. Final deprotection, air-oxidation and HPLC purification afforded the expected DTPA-conjugated CXCR4 antagonists **26a,b**. This concise protocol facilitates the selection of chelating structure and position(s) on the peptide chain, and aids structure–activity relationship studies aimed at exploring the more potent peptide probes. For example, a 4-fluorobenzoyl modification at the N-terminus, which should increase CXCR4 antagonism,[28] was easily appended to the peptide using this protocol to give the modified peptide **26c**. The subsequent treatment with nonradioactive $InCl_3$ in acidic conditions provided the In-DTPA-labeled CXCR4 antagonists **27a–c**.

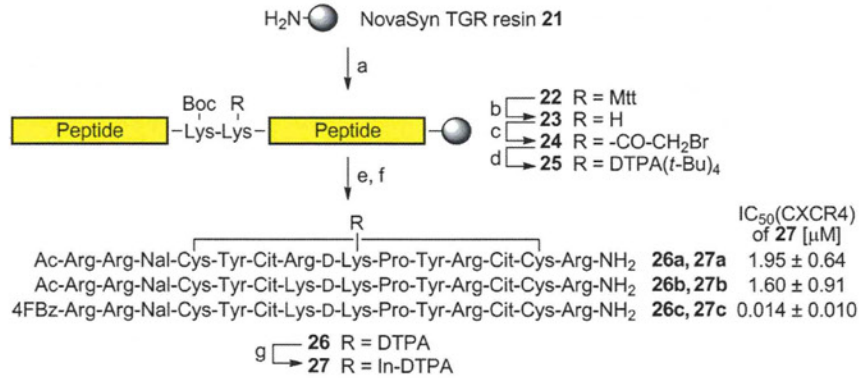

Scheme 4. Site-specific In-DTPA labeling of CXCR4 antagonists and biological activity. Reagents: (a) Fmoc-based peptide synthesis; (b) CH_2Cl_2/1,1,1,3,3,3-hexafluoro-2-propanol (HFIP)/2,2,2-trifluoroethanol (TFE)/triethylsilane (TES) (65:20:10:5); (c) $BrCH_2CO_2H$, DIC; (d) **8**, $(i\text{-}Pr)_2NEt$; (e) TFA/H_2O/EDT (95:2.5:2.5); (f) NH_4OH (air oxidation); (g) $InCl_3$. *Abbreviations:* Mtt: 4-methyltrityl; Cit: L-citrulline, Nal: L-3-(2-naphthyl)alanine, 4FBz: 4-fluorobenzoyl.

2.3. Bioactivity of In-DTPA-labeled CXCR4 antagonists

The biological activity of the In-DTPA-labeled peptides **27a–c** was evaluated as the inhibitory potency of [^{125}I]-SDF-1-binding to CXCR4 membrane extracts (Scheme 4). Peptides **27a,b**, with an N-terminal acetyl group, exhibited similar potency towards CXCR4 [IC_{50}(**27a**) = 1.95 ± 0.64 μM, IC_{50}(**27b**) = 1.60 ± 0.91 μM], indicating that the Lys and Arg for the *i*-position of β-turn were both tolerant to the bioactivity. In contrast, peptide **27c** exerted much more potent inhibitory activity for the SDF-1 binding to CXCR4 [IC_{50}(**27c**) = 0.014 ± 0.010 μM]. These results of In-DTPA-labeled peptides **27a–c** coincided with our previous report on the unlabeled peptides.[28] The novel potent In-DTPA-labeled CXCR4 antagonist **27c** could be a promising imaging probe for CXCR4-expressing malignant cancer cells.[11]

3. Conclusions

In this study, we have established a novel synthetic method for the production of DTPA–peptide conjugates. The process includes facile solid-phase synthesis of a DTPA framework using a novel precursor substrate and site-specific conjugation using a highly acid-labile protecting group. Using a temporary Ns protecting group, the DTPA precursor **8** was obtained through two purification steps from commercially available diethylenetriamine. In addition, the on-resin incorporation of a bromoacetyl group into the specific free amino group followed by the addition of the nucleophilic DTPA precursors provided the expected DTPA–peptide conjugates with high purity. Taking advantage of secondary amine precursors of choice, these processes represent versatile methods to prepare a series of peptide conjugates, including DTPA and DOTA, for optimization of imaging probes. This conjugation method was applied to the preparation of DTPA-conjugates of octreotide and CXCR4 antagonist, which have been reported to effectively detect cancer cells. The peptide **27c** with highly potent inhibitory activity of SDF-1 binding to CXCR4 was obtained without any amino acid substitution to avoid multiple modifications on the amino groups. This peptide represents a promising lead compound as an imaging probe towards CXCR4-positive metastatic tumors.

4. Experimental

4.1. Synthesis

4.1.1. Bis(*tert*-butyl) 3,6-bis[(*tert*-butoxycarbonyl)methyl]-9-(*o*-nitrobenzenesulfonyl)-3,6,9-triazaundecanedioate (14a)

To diethylenetriamine **5** (0.540 mL, 5.00 mmol) in dehydrated EtOH (5 mL), *o*-NsCl (0.367 g, 1.67 mmol) was slowly added below 0 °C. After stirring for 2 h, EtOH was removed in vacuo. To dehydrated DMF (8 mL), K_2CO_3 (4.49 g, 32.5 mmol) and $BrCH_2CO_2t$-Bu (4.06 mL, 27.5 mmol) were added at 0 °C. The mixture was stirred overnight at room temperature, and filtered. The filtrate was concentrated under reduced pressure to give an oily residue, and the residue was dissolved in EtOAc (100 mL). The whole mixture was washed with saturated $NaHCO_3$, and was dried over $MgSO_4$. Concentration under reduced pressure followed by flash chromatography over silica gel with *n*-hexane–EtOAc gave compound **14a** as a yellow oil (0.81 g, 65%); ^{1}H NMR ($CDCl_3$, 500 MHz) δ 8.08–8.11 (1H, m), 7.64–7.69 (2H, m), 7.56–7.60 (1H, m), 4.24 (2H, s), 3.49 (2H, t, *J* = 6.9 Hz), 3.42 (4H, s), 3.30 (2H, s), 2.88 (2H, t, *J* = 6.6 Hz), 2.78 (2H, t, *J* = 6.9 Hz), 2.77 (2H, t, *J* = 6.9 Hz), 1.45 (27H, s), 1.36 (9H, s); ^{13}C NMR ($CDCl_3$, 500 MHz) δ 170.6 (3C), 168.0, 133.7, 133.2, 131.6 (2C), 130.9, 123.9, 82.0, 81.0, 80.9 (2C), 56.1 (3C), 53.3, 52.8, 52.4, 49.4, 46.7, 28.1 (9C), 27.9 (3C); HRMS (FAB) *m*/*z* calcd for $C_{34}H_{58}N_4O_{12}S$ ([M+H]$^+$): 746.3772, found 746.3779.

4.1.2. Bis(*tert*-butyl) 3,6-bis[(*tert*-butoxycarbonyl)methyl]-3,6,9-triazaundecanedioate (8)

To a solution of compound **14a** (0.216 g, 0.29 mmol) in DMF (0.726 mL), LiOH (0.128 g, 2.90 mmol) and mercaptoacetic acid (0.101 mL, 1.45 mmol) were added below 0 °C. After stirring for 2 h at room temperature, the mixture was concentrated under reduced pressure, and the residue was dissolved in $CHCl_3$. The whole reaction mixture was washed with saturated $NaHCO_3$, and was dried over Na_2SO_4. Concentration under reduced pressure followed by flash chromatography over silica gel with $CHCl_3$–MeOH gave compound **8** as a yellow oil (0.124 g, 77%); ^{1}H NMR ($CDCl_3$, 500 MHz) δ 3.39 (4H, s), 3.28 (4H, s), 2.72–2.82 (6H, m), 2.63 (2H, t, *J* = 5.4 Hz), 1.39 (9H, s), 1.38 (27H, s); ^{13}C NMR ($CDCl_3$, 500 MHz) δ 170.9, 170.7 (3C), 80.8 (4C), 55.9 (2C), 55.8 (2C), 52.4, 52.3, 51.3, 47.0, 28.2 (3C), 28.1 (9C); HRMS (FAB) *m*/*z* calcd for $C_{28}H_{54}N_3O_8$ ([M+H]$^+$): 560.3911, found 560.3910.

4.1.3. Standard procedure for solid-phase peptide synthesis

Protected peptide-resins were manually constructed by Fmoc-based solid-phase peptide synthesis. *t*-Bu ester for Asp and Glu; 2,2,4,6,7-pentamethyldihydrobenzofurane-5-sulfonyl (Pbf) for Arg; *t*-Bu for Thr and Tyr; Boc for Lys and Trp; Trt for Cys were employed for side-chain protection. Fmoc-amino acids were coupled using three equivalents of reagents [Fmoc-amino acid, 1,3-diisopropylcarbodiimide (DIC), and HOBt·H_2O] to the free amino group in DMF for 1.5 h. Fmoc deprotection was performed by 20% (v/v) piperidine in DMF (2 × 1 min, 1 × 30 min). The protected peptide resin was treated with a cocktail of deprotection reagents. After removal of the resin by filtration, the filtrate was poured into ice-cold dry Et_2O. The resulting powder was collected by centrifugation and washed with ice-cold dry Et_2O. The crude peptide was dissolved in H_2O, and the pH was adjusted to 8.0 with NH_4OH for disulfide bond formation. After air-oxidation for 1 d, the crude product was purified by preparative HPLC on a Cosmosil 5C18-ARII preparative column (Nacalai Tesque, Kyoto, Japan; 20 × 250 mm, flow rate 10 mL/min) to afford the expected peptides. All peptides were characterized by MALDI-TOF-MS (AXIMA-CFR plus, Shimadzu, Kyoto, Japan) and the purity was calculated as >95% by HPLC on a Cosmosil 5C18-ARII analytical column (Nacalai Tesque, 4.6 × 250 mm, flow rate 1 mL/min) at 220 nm absorbance.

4.1.4. Preparation of DTPA- and DOTA-conjugated octreotides (19a,b)

According to the procedure reported previously,[18] (2-chloro)trityl chloride resin **15** (214 mg, 1.4 mmol/g), Fmoc-Thr(*t*-Bu)-ol (345 mg, 0.9 mmol), and pyridine (0.145 mL, 1.8 mmol) were agitated for 21 h in dry CH_2Cl_2–DMF (1:1, 3.94 mL). The loading was determined by measuring the 290 nm UV absorption of the piperidine-treated sample (0.455 mmol/g). After the construction of the peptide chain (0.017 mmol scale) using a standard procedure, bromoacetic acid (23.6 mg, 0.17 mmol) with DIC (0.026 mL, 0.17 mmol) in CH_2Cl_2 was reacted with resin **16** for 2 h at room temperature. The subsequent treatment of **17** with amines **8** (29.0 mg, 0.51 mmol) and **20** (26.3 mg, 0.51 mmol) with $(i\text{-Pr})_2$NEt (0.009 mL, 0.51 mmol) in DMF for 12 h at room temperature provided **18a** and **18b**, respectively. Cleavage and deprotection of **18a** (72.5 mg) and **18b** (73.8 mg) was achieved using a TFA/1,2-ethandithiol (EDT)/H_2O (5 mL; 95:2.5:2.5) cocktail for 2 h at room temperature and by treatment with 1 M TMSBr-thioanisole/TFA in the presence of EDT/*m*-cresol (3.3 mL) for 2 h at 0 °C, respectively. After disulfide formation under air-oxidation conditions, the crude peptides were purified using the standard procedure, to afford the desired peptides **19a** (8.2 mg, 23%) and **19b** (9.5 mg, 26%) as white powders. Compound **19a**: MS (MALDI-TOF) *m*/*z* calcd for $C_{63}H_{89}N_{13}O_{19}S_2$ ([M+H]$^+$): 1395.6, found 1395.3. Compound **19b**:

MS (MALDI-TOF) m/z calcd for $C_{65}H_{93}N_{14}O_{17}S_2$ ($[M+H]^+$): 1405.6, found 1405.8.

4.1.5. Preparation of DTPA-conjugated CXCR4 antagonists (26a–c)

Protected peptide resins were manually constructed according to the standard procedure using NovaSyn TGR-resin **21** (96.2 mg, 0.025 mmol). 4-Methyltrityl (Mtt) group was employed for the protection of the D-Lys ε-amino group. The N-terminal amino group was acylated by treatment with Ac_2O (0.012 mL, 0.125 mmol)/pyridine (0.020 mL, 0.250 mmol) for 1 h at room temperature for peptides **26a,b**, and with 4-fluorobenzoic acid (17.5 mg, 0.125 mmol)/DIC (0.019 mL, 0.125 mmol)/HOBt·H_2O (19.2 mg, 0.125 mmol) for 1.5 h at room temperature for peptide **26c**. Subsequently, the resin **22** was treated with CH_2Cl_2/1,1,1,3,3,3-hexafluoropropan-2-ol (HFIP)/trifluoroethanol (TFE)/triethylsilane (TES) [65:20:10:5; 5 mL] for 2 h at room temperature. The DTPA group was incorporated using the identical procedure employed for the synthesis of the octreotide derivative **19a**. Treatment of the resins (**25a**: 178 mg, **25b**: 165 mg, **25c**: 162 mg) with a TFA/1,2-ethandithiol(EDT)/H_2O (95:2.5:2.5; 5 mL) cocktail for 2 h at room temperature followed by air oxidation and purification provided the peptides Compound **26a** (14.6 mg, 15.4%), **26b** (6.67 mg, 8.7%) and **26c** (7.4 mg, 9.5%) as white powders. Compound **26a:** MS (MALDI-TOF) m/z calcd for $C_{106}H_{165}N_{38}O_{28}S_2$ ($[M+H]^+$): 2482.2, found 2482.5. Compound **26b**: MS (MALDI-TOF) m/z calcd for $C_{106}H_{165}N_{36}O_{28}S_2$ ($[M+H]^+$): 2454.2, found 2453.9. Compound **26c**: MS (MALDI-TOF) m/z calcd for $C_{111}H_{166}FN_{36}O_{28}S_2$ ($[M+H]^+$): 2534.2, found 2533.8.

4.1.6. Indium chelating for CXCR4 antagonist probes (27a–c)

To a solution of peptides **26a–c** (8 mM in 0.1 N AcOH, **26a**: 45.9 μL, 0.37 μmol; **26b**: 48.4 μL, 0.39 μmol; **26c**: 48.8 μL, 0.39 μmol), $InCl_3$ (1 M in 0.02 N HCl, 50 μL) was added and the solution stirred for a further 30 min at room temperature. HPLC purification using a standard procedure provided the desired peptides **27a** (0.43 mg, 36.7%), **27b** (0.42 mg, 34.3%) and **27c** (0.38 mg, 30.3%) as white powders. Compound **27a**: MS (MALDI-TOF) m/z calcd for $C_{106}H_{165}InN_{38}O_{28}S_2$ ($[M+H]^+$): 2597.1, found 2596.9. Compound **27b**: MS (MALDI-TOF) m/z calcd for $C_{106}H_{165}InN_{36}O_{28}S_2$ ($[M+H]^+$): 2569.1, found 2569.1. Compound **27c**: MS (MALDI-TOF) m/z calcd for $C_{111}H_{166}FInN_{36}O_{28}S_2$ ($[M+H]^+$): 2649.1, found 2649.0.

4.2. Evaluation of [^{125}I]-SDF-1 binding and displacement

For ligand binding, the CXCR4 membrane was incubated with 0.5 nM of [^{125}I]-SDF-1 and increasing concentrations of compounds **27a–c** in binding buffer [50 mM HEPES (pH 7.4), 5 mM $MgCl_2$, 1 mM $CaCl_2$ and 0.1% BSA in H_2O] for 1 h at room temperature. The reaction mixtures were filtered through GF/B filters (Perkin-Elmer, Wellesley, MA) pretreated with 0.1% polyethyleneimine. The filter plate was washed with wash buffer [50 mM HEPES (pH 7.4), 500 mM NaCl and 0.1% BSA in H_2O] and the bound radioactivity was measured by TopCount (Packard, Meriden, CT). Inhibitory activity of test compounds was determined based on the inhibition of [^{125}I]-SDF-1 binding to the CXCR4 receptor (IC_{50}).

Acknowledgments

This work is supported by Grants-in-Aid for Scientific Research and Molecular Imaging Research Program from the Ministry of Education, Culture, Sports, Science, and Technology of Japan. R.M. is grateful for Research Fellowships from the JSPS for Young Scientists.

Supplementary data

Supplementary data associated with this article can be found, in the online version, at doi:10.1016/j.bmc.2011.03.059.

References and notes

1. Lee, S.; Xie, J.; Chen, X. *Chem. Rev.* **2010**, *110*, 3087.
2. De León-Rodríguez, L. M.; Kovacs, Z. *Bioconjugate Chem.* **2008**, *19*, 391.
3. Mier, W.; Hoffend, J.; Krmer, S.; Schuhmacher, J.; Hull, W. E.; Eisenhut, M.; Haberkorn, U. *Bioconjugate Chem.* **2005**, *16*, 237.
4. Lewis, M. R.; Shively, J. E. *Bioconjugate Chem.* **1998**, *9*, 72.
5. Heppeler, A.; Froidevaux, S.; Mäcke, H. R.; Jermann, E.; Powell, P.; Henning, M. *Chem. Eur. J.* **1999**, *5*, 1974.
6. De León-Rodriguez, L. M.; Kovacs, Z.; Dieckmann, G. R.; Sherry, A. D. *Chem. Eur. J.* **2004**, *10*, 1149.
7. Wild, D.; Wicki, A.; Mansi, R.; Béhé, M.; Keil, B.; Bernhardt, P.; Christofori, G.; Ell, P. J.; Mäcke, H. R. *J. Nucl. Med.* **2010**, *51*, 1059, and the references therein.
8. De Jong, M.; Breeman, W. A.; Bakker, W. H.; Kooij, P. P.; Bernard, B. F.; Hofland, L. J.; Visser, T. J.; Srinivasan, A.; Schmidt, M. A.; Erion, J. L.; Bugaj, J. E.; Mäcke, H. R.; Krenning, E. P. *Cancer Res.* **1998**, *58*, 437.
9. Hnatowich, D. J.; Layne, W. W.; Childs, R. L. *Int. J. Appl. Radiat. Isot.* **1982**, *33*, 327.
10. Wang, S.; Luo, J.; Lantrip, D. A.; Waters, D. J.; Mathias, C. J.; Green, M. A.; Fuchs, P. L.; Low, P. S. *Bioconjugate Chem.* **1997**, *8*, 673.
11. Reilly, R.; Lee, N.; Houle, S.; Law, J.; Marks, A. *Appl. Radiat. Isot.* **1992**, *43*, 961.
12. Hnatowich, D. J.; Layne, W. W.; Childs, R. L.; Lanteigne, D.; Davis, M. A.; Griffin, T. W.; Doherty, P. W. *Science* **1983**, *220*, 613.
13. Van Hagen, P. M.; Breeman, W. A. P.; Bernard, H. F.; Schaar, M.; Mooij, C. M.; Srinivasan, A.; Schmidt, M. A.; Krenning, E. P.; De Jong, M. *Int. J. Cancer* **2000**, *90*, 186.
14. Arano, Y.; Uezono, T.; Akizawa, H.; Ono, M.; Wakisaka, K.; Nakayama, M.; Sakahara, H.; Konishi, J.; Yokoyama, A. *J. Med. Chem.* **1996**, *39*, 3451.
15. A portion of this study was reported in a preliminary communication: Masuda, R.; Ohno, H.; Oishi, S.; Fujii, N. In *Pepide Science*, Okamoto, Ed.; 2009, p 159.
16. Peterson, J. J.; Pak, R. H.; Meares, C. F. *Bioconjugate Chem.* **1999**, *10*, 316.
17. Hidai, Y.; Kan, T.; Fukuyama, T. *Chem. Pharm. Bull.* **2000**, *48*, 1570.
18. Arano, Y.; Akizawa, H.; Uezono, T.; Akaji, K.; Ono, M.; Funakoshi, S.; Koizumi, M.; Yokoyama, A.; Kiso, Y.; Saji, H. *Bioconjugate Chem.* **1997**, *8*, 442.
19. Lewis, J. S.; Anderson, C. J. *Methods Mol. Biol.* **2007**, *386*, 227.
20. Albert, R.; Smith-Jones, P.; Stolz, B.; Simeon, C.; Knecht, H.; Bruns, C.; Pless, J. *Bioorg. Med. Chem. Lett.* **1998**, *8*, 1207.
21. Müller, A.; Homey, B.; Soto, H.; Ge, N.; Catron, D.; Buchanan, M. E.; McClanahan, T.; Murphy, E.; Yuan, W.; Wagner, S. N.; Barrera, J. L.; Mohar, A.; Verástegui, E.; Zlotnik, A. *Nature* **2001**, *410*, 50.
22. Hermann, P. C.; Huber, S. L.; Heeschen, C. *Cell Cycle* **2008**, *7*, 188.
23. Oishi, S.; Masuda, R.; Evans, B.; Ueda, S.; Goto, Y.; Ohno, H.; Hirasawa, A.; Tsujimoto, G.; Wang, Z.; Peiper, S. C.; Naito, T.; Kodama, E.; Matsuoka, M.; Fujii, N. *ChemBioChem* **2008**, *9*, 1154.
24. Nishizawa, K.; Nishiyama, H.; Oishi, S.; Tanahara, N.; Kotani, H.; Mikami, Y.; Toda, Y.; Evans, B. J.; Peiper, S. C.; Saito, R.; Watanabe, J.; Fujii, N.; Ogawa, O. *Int. J. Cancer* **2010**, *127*, 1180.
25. Hanaoka, H.; Mukai, T.; Tamamura, H.; Mori, T.; Ishino, S.; Ogawa, K.; Iida, Y.; Doi, R.; Fujii, N.; Saji, H. *Nucl. Med. Biol.* **2006**, *33*, 489.
26. Tamamura, H.; Omagari, A.; Oishi, S.; Kanamoto, T.; Yamamoto, N.; Peiper, S. C.; Nakashima, H.; Otaka, A.; Fujii, N. *Bioorg. Med. Chem. Lett.* **2000**, *10*, 2633.
27. Stephenson, K. A.; Banerjee, S. R.; McFarlane, N.; Boreham, D. R.; Maresca, K. P.; Babich, J. W.; Zubieta, J.; Valliant, J. F. *Can. J. Chem.* **2005**, *83*, 2060.
28. Tamamura, H.; Hiramatsu, K.; Mizumoto, M.; Ueda, S.; Kusano, S.; Terakubo, S.; Akamatsu, M.; Yamamoto, N.; Trent, J. O.; Wang, Z.; Peiper, S. C.; Nakashima, H.; Otaka, A.; Fujii, N. *Org. Biomol. Chem.* **2003**, *1*, 3663.

Journal of Medicinal Chemistry

Article

pubs.acs.org/jmc

Structure–Activity Relationship Study of a CXC Chemokine Receptor Type 4 Antagonist, FC131, Using a Series of Alkene Dipeptide Isosteres

Kazuya Kobayashi,[†] Shinya Oishi,*[,†] Ryoko Hayashi,[†] Kenji Tomita,[†] Tatsuhiko Kubo,[†] Noriko Tanahara,[†] Hiroaki Ohno,[†] Yasushi Yoshikawa,[‡] Toshio Furuya,[‡] Masaru Hoshino,[†] and Nobutaka Fujii*[,†]

[†]Graduate School of Pharmaceutical Sciences, Kyoto University, Sakyo-ku, Kyoto 606-8501, Japan

[‡]PharmaDesign Inc., Chuo-ku, Tokyo 104-0032, Japan

Supporting Information

ABSTRACT: A structure–activity relationship study on a highly potent CXC chemokine receptor type 4 (CXCR4) antagonist, FC131 [cyclo(-D-Tyr[1]-Arg[2]-Arg[3]-Nal[4]-Gly[5]-)], was carried out using a series of alkene isosteres of the D-Tyr[1]-L/D-Arg[2] dipeptide to investigate the binding mode of FC131 and its derivatives with CXCR4. The structure–activity relationships of isostere-containing FC131 analogues were similar to those of the parent FC131 and its derivatives, suggesting that a *trans*-conformer of the D-Tyr[1]–Arg[2] peptide bond is the dominant contributor to the bioactive conformations of FC131. Although NMR analysis demonstrated that the two conformations of the peptidomimetic containing the D-Tyr[1]-D-Arg[2] isostere are possible, binding-mode prediction indicated that the orientations of the alkene motif within D-Tyr[1]-MeArg[2] peptidomimetics depend on the chirality of Arg[2] and the β-methyl group of the isostere unit, which makes the dominant contribution for binding to the receptor. The most potent FC122 [cyclo(-D-Tyr[1]-D-MeArg[2]-Arg[3]-Nal[4]-Gly[5]-)] bound with CXCR4 by a binding mode different from that of FC131.

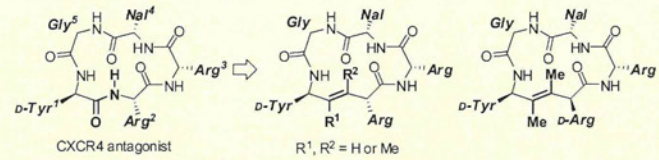

INTRODUCTION

Cyclic peptides provide versatile scaffolds for the development of therapeutic agents in drug discovery from peptide ligands.[1] The cyclic structure provides several advantages, including preorganized conformations to improve the affinity for the target molecule(s),[2] protection from proteolytic degradation by exopeptidases,[3] and increased membrane permeability.[4,5] The restricted conformations can facilitate the identification of preferred spatial distributions of functional groups necessary for bioactivity. Cyclic peptides therefore offer promising lead compounds for optimization of small-molecule ligands via improvement of the bioactivity and/or selectivity in ligand-based drug design.[6] For example, Kessler and co-workers developed a cyclic RGD pentapeptide for highly potent antagonists of $\alpha_v\beta_3$ integrin.[7] The subsequent structure–activity relationship (SAR) studies identified a more potent and selective cyclic peptide.[8] Using information on the spatial distributions of the pharmacophoric elements of cyclic RGD peptides, small-molecule inhibitors with a variety of druglike scaffolds have been developed.[9−12] Endothelin receptor antagonists,[13−15] endomorphin-1 analogues,[16,17] and somatostatin analogues[18,19] with cyclic peptide scaffolds have also been exemplified.

Previously, we developed a highly potent CXC chemokine receptor type 4 (CXCR4) antagonist, FC131 [cyclo(-D-Tyr[1]-Arg[2]-Arg[3]-Nal[4]-Gly[5]-)], from a library of cyclic pentapeptides consisting of pharmacophore residues of the polyphemusin-II-derived anti-human immunodeficiency virus (HIV) peptide T140.[20] Since this novel scaffold for CXCR4 antagonists was identified, a series of cyclic peptides and peptidomimetics have been designed for potential anti-HIV and antimetastatic agents.[21] For example, substitution of Arg[2] in FC131 with D-Arg and/or *N*-methylarginine (MeArg) provided interesting insights into SARs:[22] (1) the D-Arg[2]-substituted derivative (FC092) showed slightly less potent activity than FC131 did, (2) in the low-energy structures of FC092, the orientation of the D-Tyr[1]–D-Arg[2] peptide bond was flipped (Figure 1a,b), (3) the MeArg[2]-substituted peptide (FC162) is less potent than FC131 is, (4) the D-MeArg[2]-substituted peptide (FC122) is the most potent, and approximately 30% of the *N*-methylamide bonds in D-Tyr[1]-D-MeArg[2] exist as the *cis*-conformer, and (5) the local conformation around D-Tyr[1]-D-MeArg[2] in FC122 is similar to that of FC131 (Figure 1a,c). The D-Tyr[1]-Arg[2] substructure in FC131 is therefore involved in direct or indirect contributions to binding with CXCR4. The different biological effects among the derivatives are likely to be derived from two possible pseudo-1,3-allylic strains between the Arg[2] side chain and the D-Tyr[1] carbonyl group and between the D-Tyr[1] side chain and the *N*-methyl group of MeArg[2]; these can affect the orientations of the peptide bond (Figure 1b,c). In this study, we investigated the electrostatic and steric effects around

Received: December 15, 2011
Published: February 21, 2012

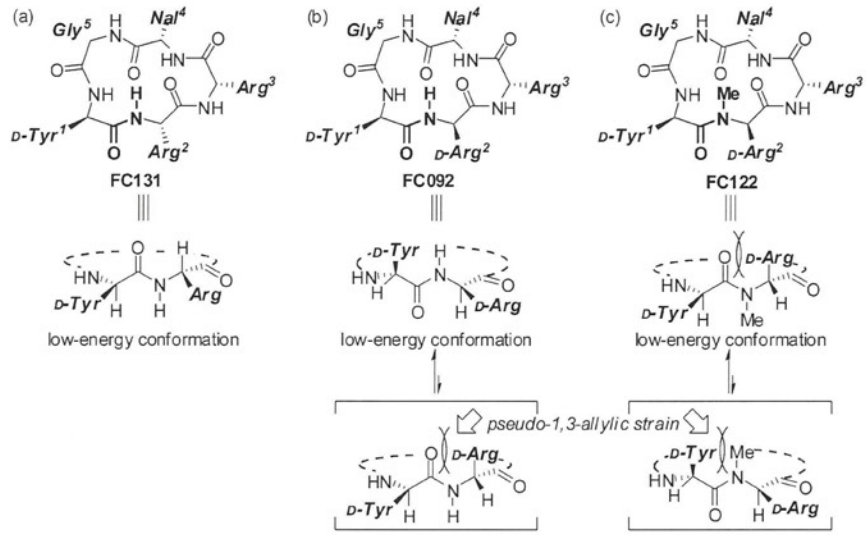

Figure 1. Structures of cyclic pentapeptide CXCR4 antagonists and the bioactivity-relevant peptide bond orientations in D-Tyr-L-Arg in FC131 (a), D-Tyr-D-Arg in FC092 (b), and D-Tyr-D-MeArg in FC122 (c). Nal = L-3-(2-naphthyl)alanine.

the D-Tyr[1]-Arg[2] substructure using a series of alkene dipeptide isosteres. Computational analysis was also performed to assess the binding mode to CXCR4 of FC131 and its derivatives.

RESULTS AND DISCUSSION

Design and Synthesis of a Series of FC131 Derivatives Containing Alkene Dipeptide Isosteres. Peptide bonds constitute the assembly units for secondary and tertiary structures as well as the functional motifs for intermolecular interactions with binding partners via hydrogen bond acceptor/donor properties. Because replacement of peptide bonds with isosteric mimetics is one of the usual practices in performing SAR studies on bioactive and functional peptides, a number of peptide bond isosteres have been developed and used in medicinal chemistry. To identify the dominant conformations that contribute to the bioactivity of FC131 derivatives, alkene dipeptide isosteres were used for the SAR study (Figure 2). A planar alkene motif can restrict the possible *cis*/*trans* isomerization of peptide bonds.[23−25] In the trisubstituted alkene isosteres,[26,27] a γ-methyl group serves as a substituent corresponding to the carbonyl oxygen of a peptide bond. Tetrasubstituted alkene isosteres mimic *N*-methylamide bonds.[28] Our expectation was that, using a series of alkene isosteres, the steric effects of the carbonyl group and *N*-methyl group of the D-Tyr−Arg peptide bond on the peptide conformation and bioactivity could be understood. The contributions of the D-Tyr−Arg peptide bond to the hydrogen-bonding interactions could also be revealed by replacement with the isosteres because these substituted alkene motifs cannot engage in dipole interactions (Figure 3).

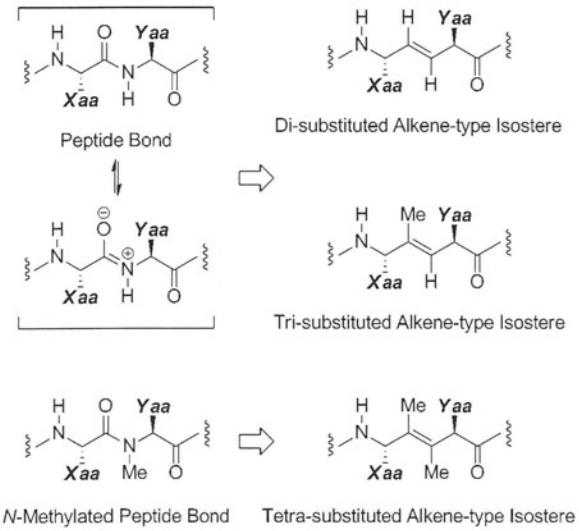

Figure 2. Structures of a series of alkene dipeptide isosteres. Xaa and Yaa = amino acid side chains.

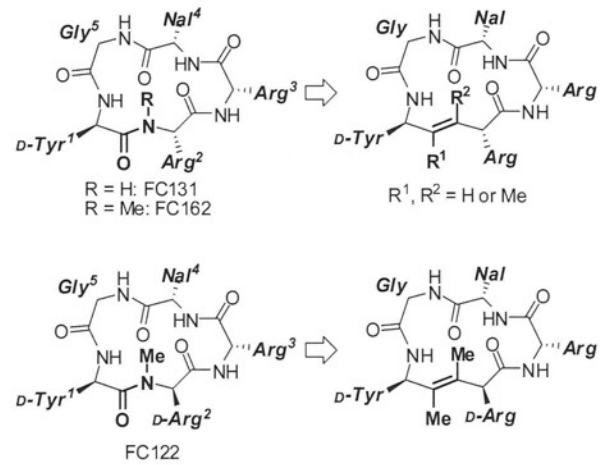

Figure 3. Design of alkene isostere-containing derivatives of cyclic pentapeptide-based CXCR4 antagonists. Nal = L-3-(2-naphthyl)-alanine.

For the coupling component in the solid-phase peptide synthesis, a fully protected D-Tyr-Orn isostere, **10** (Orn = L-ornithine), was designed in which the Orn δ-amino group can be converted into an Arg guanidino group after peptide synthesis.[29,30] A synthetic method for disubstituted alkene dipeptide isosteres has previously been reported.[31] Initially, the D-tyrosine derivative **1** was converted to *syn*-allyl alcohol **2** by a one-pot reduction and vinylation (Scheme 1). After protection of the hydroxyl group of **2** with an acetyl group, ozonolysis and

dx.doi.org/10.1021/jm2016914 | J. Med. Chem. 2012, 55, 2746−2757

Scheme 1[a]

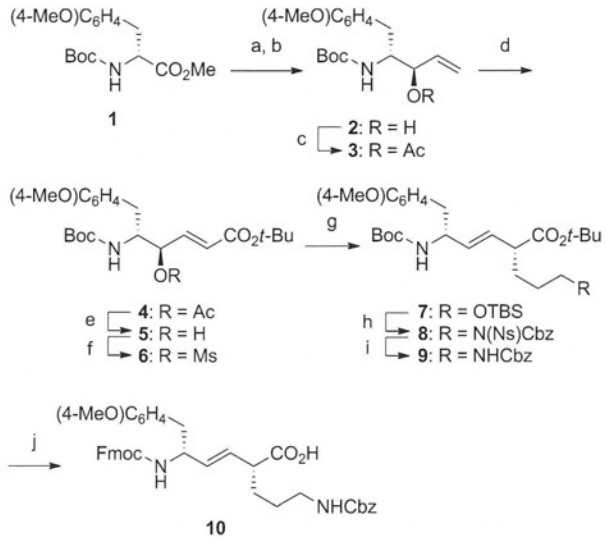

[a]Reagents and conditions: (a) DIBAL-H, CH_2Cl_2–toluene, −78 °C, 20 min, then $H_2C{=}CHMgBr$, $ZnCl_2$, LiCl, THF, −78 °C, 3 h (31%); (b) recrystallization; (c) Ac_2O, pyridine, DMAP, $CHCl_3$, 0 °C, 2 h (quantitative); (d) (i) O_3, EtOAc, −78 °C, then Me_2S, 0 °C, 30 min; (ii) $(EtO)_2P(O)CH_2CO_2$-*t*-Bu, LiCl, $(i\text{-}Pr)_2NEt$, MeCN, 0 °C, 3 h (62%); (e) K_2CO_3, MeOH, rt, 2 h (96%); (f) MsCl, Et_3N, CH_2Cl_2, 0 °C, 2 h (96%); (g) $TBSO(CH_2)_3Li$, CuCN, LiCl, THF–Et_2O–*n*-pentane, −78 °C, 30 min (94%); (h) (i) H_2SiF_6(aq), MeCN–H_2O, rt, 2 h; (ii) NsNH(Cbz), DEAD, PPh_3, THF–toluene, 0 °C, 3 h (86%); (i) PhSH, K_2CO_3, DMF, rt, 3 h (96%); (j) (i) TFA, CH_2Cl_2, rt, 2 h; (ii) FmocOSu, Et_3N, MeCN–H_2O, rt, 2 h (71%).

a subsequent Horner–Wadsworth–Emmons reaction (HWE reaction) afforded an (*E*)-isomer of *α,β*-enoate **4**. Alcoholysis of the acetyl group followed by mesylation yielded *γ*-(mesyloxy)-*α,β*-enoate **6**, which is a key substrate for organocopper-mediated S_N2' alkylations. Treatment of **6** with $TBSO(CH_2)_3Li$ in the presence of CuCN and LiCl gave an *α*-alkylated product, **7**. The side chain silyl ether group in **7** was converted to a Cbz-protected amino group via a Mitsunobu reaction using NsNH(Cbz). Removal of Ns, Boc and *t*-Bu groups, followed by *N*-Fmoc protection, provided the expected isostere component **10**.

Tri- and tetrasubstituted alkene isosteres for D-Tyr-Orn dipeptide were synthesized according to the protocol established in our previous studies.[32,33] *syn*-Allyl alcohols **12a,b** were obtained by sequential methylation and alkenylation of Weinreb amide **11** using Grignard reagents (Scheme 2). Cyclization of **12a,b** under basic conditions followed by Boc protection gave oxazolidinones **13a,b**. 5-Vinyloxazolidinone **13a** was converted to an *α,β*-unsaturated ester, **15a**, by ozonolysis and HWE reaction. In contrast, the same HWE reaction of ketone **14**, which was derived from 5-propenyloxazolidinone **13b**, did not proceed. The *β*-methylated congener **15b** was provided via Wittig reaction of **14** using $Ph_3P{=}CHCO_2$-*t*-Bu. Organocopper-mediated alkylations of **15a,b** gave the *anti*-S_N2' products **16a,b** with moderate (*E*)-selectivity. Although the (*E*)- and (*Z*)-isomers of **16a** were not separated in this step, the (*E*)-isomer of alcohol **17a** was isolated by column chromatography. Alcohols **17a,b** were converted to the desired Fmoc-protected amino acids **20a,b** using methods identical to those described for the synthesis of **10**.

Scheme 2[a]

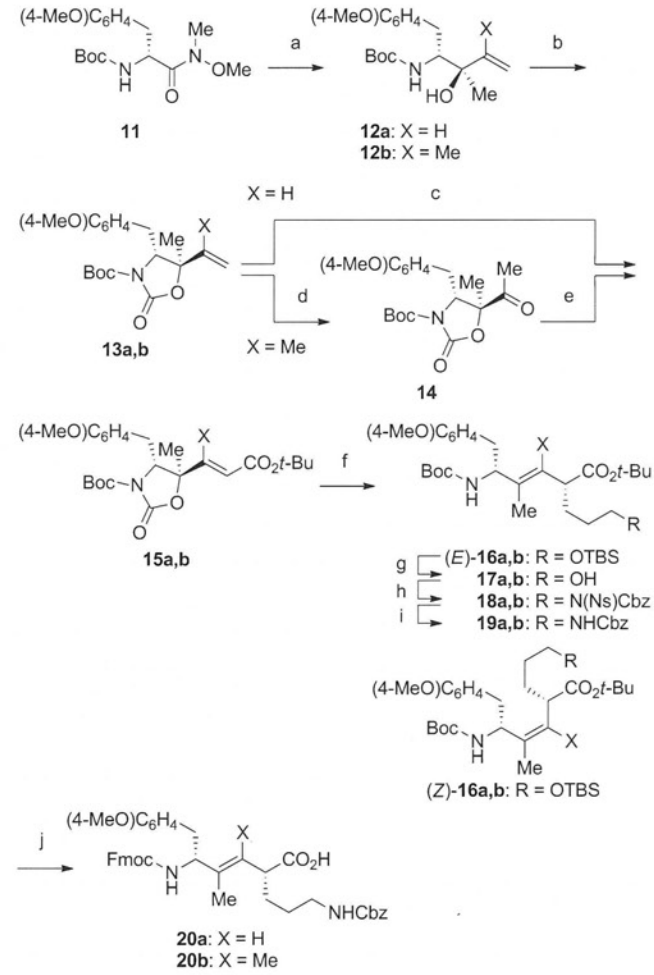

[a]Reagents and conditions: (a) (i) MeMgCl, THF, −78 °C, 1.5 h; (ii) $CH_2{=}CXMgBr$, $CeCl_3$, THF, 0 °C, 3 h; (iii) recrystallization (**12a**, 48%; **12b**, 47%); (b) NaH, THF, reflux, 1 h, then $(Boc)_2O$, rt, 2 h (**13a**, quantitative; **13b**, 87%); (c) (i) O_3, EtOAc, −78 °C, then Me_2S, −78 °C, 30 min; (ii) $(EtO)_2P(O)CH_2CO_2$-*t*-Bu, LiCl, $(i\text{-}Pr)_2NEt$, MeCN, 0 °C, 3.5 h (56%); (d) O_3, EtOAc, −78 °C, then Me_2S, −78 °C, 15 min (99%); (e) $Ph_3P{=}CHCO_2$-*t*-Bu, toluene, reflux, 10 h (quantitative); (f) $TBSO(CH_2)_3Li$, CuCN, LiCl, THF–Et_2O–*n*-pentane, −78 °C, 2 h (**16a**, 92%, *E*/*Z* = 80/20; **16b**, quantitative, *E*/*Z* = 79/21); (g) H_2SiF_6(aq), MeCN–H_2O, rt, 13.5 h (**17a**, 51%; **17b**, 91%); (h) NsNH(Cbz), DEAD, PPh_3, THF–toluene, 0 °C, overnight (**18a**, 61%; **18b**, quantitative); (i) PhSH, K_2CO_3, DMF, rt, overnight (**19a**, 81%; **19b**, 84%); (j) (i) TFA, CH_2Cl_2, rt, 2 h; (ii) FmocOSu, $(i\text{-}Pr)_2NEt$, MeCN–H_2O, rt, 14.5 h (**20a**, 57%; **20b**, 90%).

The epimeric D-Tyr-D-Orn dipeptide isostere **26** was also synthesized. Although a (*Z*)-selective HWE reaction[34] or modified Wittig reaction[35] of ketone **14** failed, Peterson olefination[36,37] provided an *E*/*Z* mixture of *α,β*-unsaturated esters in moderate yield (**15b**/**21** = 3/2) (Scheme 3). The mixture was converted to three *α*-alkylated products, namely, **22**, (*E*)-**16b**, and (*Z*)-**16b**. After cleavage of the TBS group, Mitsunobu reaction, and removal of the Ns group, a mixture of **25** and **19b** was separated from the (*Z*)-product derived from (*Z*)-**16b**. The desired D-Tyr-D-Orn isostere **26** was obtained via TFA-mediated deprotection and *N*-Fmoc protection, followed by separation from **20b** by column chromatography.

A representative synthesis of the isostere-containing FC131 derivatives is shown in Scheme 4. The protected peptide resin

dx.doi.org/10.1021/jm2016914 | J. Med. Chem. 2012, 55, 2746–2757

Scheme 3[a]

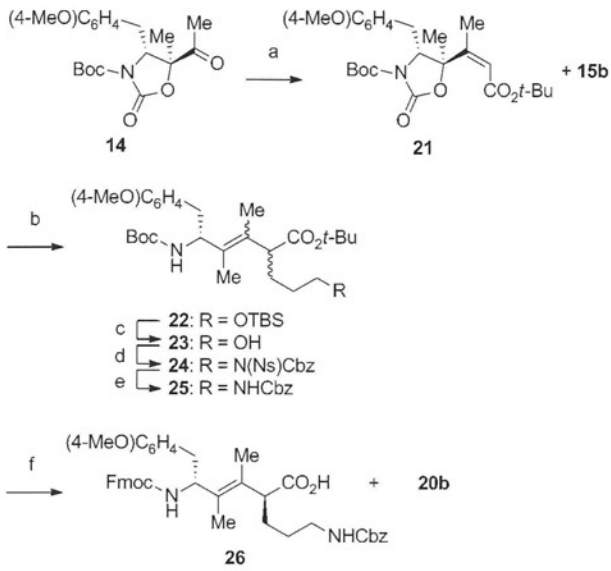

[a]Reagents and conditions: (a) $TMSCH_2CO_2$-*t*-Bu, LDA, THF–*n*-hexane, −78 °C, 4 h (53%, **15b**/**21** = 3/2); (b) $(TBS)O(CH_2)_3Li$, CuCN, LiCl, THF–Et_2O–*n*-pentane, −78 °C, 2 h (89%); (c) H_2SiF_6(aq), MeCN–H_2O, rt, 13.5 h (90%); (d) NsNH(Cbz), DEAD, PPh_3, THF–toluene, 0 °C, overnight (95%); (e) PhSH, K_2CO_3, DMF, rt, overnight (82%); (f) (i) TFA, CH_2Cl_2, rt, 2 h; (ii) FmocOSu, $(i\text{-}Pr)_2NEt$, MeCN–H_2O, rt, 14.5 h (**26**, 39%; **20b**, 54%).

Scheme 4[a]

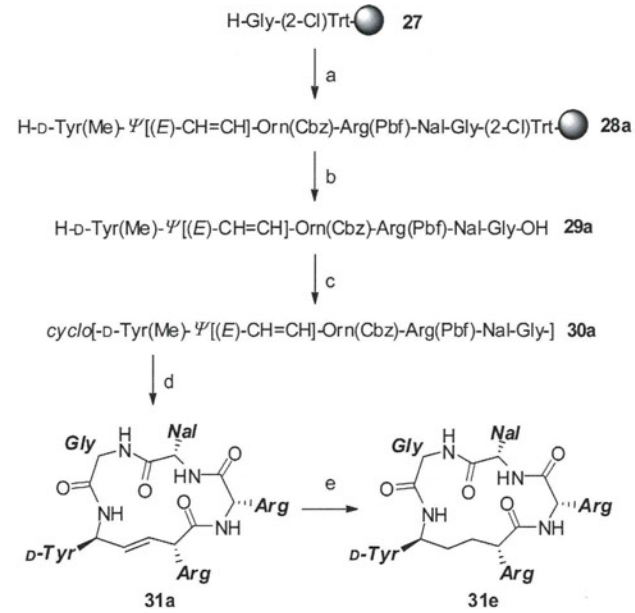

[a]Reagents and conditions: (a) Fmoc-based solid-phase peptide synthesis; (b) HFIP, CH_2Cl_2, rt, 2 h; (c) DPPA, $NaHCO_3$, DMF, −40 °C to rt, 48 h; (d) (i) TMSOTf–thioanisole in TFA, 0 °C to rt, 3.5 h; (ii) 1*H*-pyrazole-1-carboxamidine hydrochloride, Et_3N, DMF, rt, 2 days (22% from **27**); (e) H_2, Pd/$BaSO_4$, MeOH, rt, 36 h (33%).

28a was prepared on a 2-chlorotrityl [(2-Cl)Trt] resin using standard Fmoc-based solid-phase peptide synthesis. After cleavage of **28a** from the resin, the linear peptide **29a** was cyclized to **30a** using diphenylphosphoryl azide (DPPA). Removal of the side chain protecting groups in **30a** followed by conversion of the Orn δ-amino group to a guanidino group using 1*H*-pyrazole-1-carboxamidine gave the expected peptide **31a** with a D-Tyr-Arg isostere. The derivatives **31b–d** were also obtained by the same procedure. In addition, an FC131 analogue, **31e**, with a D-Tyr-Arg ethylene isostere was prepared by hydrogenation of **31a** using Pd/$BaSO_4$.

Structure–Activity Relationships of FC131 Derivatives for CXCR4 Binding. We assessed the receptor binding of cyclic peptides **31a–e** with CXCR4 for inhibitory potency against [^{125}I]stromal-cell-derived factor-1 (SDF-1) binding to CXCR4 (Table 1). The biological activities of the disubstituted

Table 1. Inhibitory Activity of FC131 Derivatives against SDF-1 Binding to CXCR4

peptide	sequence	IC_{50}[a] (μM)
FC131	cyclo(-D-Tyr^1-L-Arg^2-L-Arg^3-L-Nal^4-Gly^5-)	0.084 ± 0.037
31a	cyclo(-D-Tyr^1-ψ[(*E*)-CH=CH]-L-Arg^2-L-Arg^3-L-Nal^4-Gly^5-)	0.33 ± 0.074
31b	cyclo(-D-Tyr^1-ψ[(*E*)-CMe=CH]-L-Arg^2-L-Arg^3-L-Nal^4-Gly^5-)	0.50 ± 0.21
31c	cyclo(-D-Tyr^1-ψ[(*E*)-CMe=CMe]-L-Arg^2-L-Arg^3-L-Nal^4-Gly^5-)	2.5 ± 1.0
31d	cyclo(-D-Tyr^1-ψ[(*E*)-CMe=CMe]-D-Arg^2-L-Arg^3-L-Nal^4-Gly^5-)	0.10 ± 0.029
31e	cyclo(-D-Tyr^1-ψ[CH_2–CH_2]-L-Arg^2-L-Arg^3-L-Nal^4-Gly^5-)	>10
FC162	cyclo(-D-Tyr^1-L-MeArg^2-L-Arg^3-L-Nal^4-Gly^5-)	0.29 ± 0.12
FC122	cyclo(-D-Tyr^1-D-MeArg^2-L-Arg^3-L-Nal^4-Gly^5-)	0.063 ± 0.032

[a]IC_{50} values are the concentrations for 50% inhibition of the [^{125}I]SDF-1α binding to CXCR4 (n = 3).

alkene-containing peptide **31a** and trisubstituted alkene-containing peptide **31b** were slightly less than that of FC131. These results suggested that the hydrogen-bonding capability of the D-Tyr^1–L-Arg^2 peptide bond in FC131 is not necessary, but is partly effective. The nearly equipotent activities of **31a** and **31b** indicated that the steric effects of a γ-methyl group of the alkene isostere in **31b**, which corresponds to the D-Tyr^1 carbonyl oxygen of FC131, are not critical to the antagonistic activity. Peptide **31c** containing a tetrasubstituted alkene isostere for D-Tyr^1-L-MeArg^2 exhibited low activity, whereas the D-MeArg^2 congener **31d** showed activity nearly equipotent to that of FC131. The bioactivity profile of the isostere-containing peptides was similar to that of a series of the parent peptides, including FC162 and FC122, except that their potencies were somewhat lower than those of the parents. These observations suggested that the *trans*-isomer of the D-Tyr^1–L/D-Arg^2 peptide bond contributes to the bioactivity of FC131 and its derivatives and that tri- and tetrasubstituted alkene isosteres closely mimic the D-Tyr^1-L-Arg^2 dipeptide and *N*-methylated congeners (D-Tyr^1-L-MeArg^2 and D-Tyr^1-D-MeArg^2), respectively. On the other hand, an ethylene isostere-containing analogue, **31e**, did not bind with CXCR4. The increased flexibility of the peptide backbone as a result of the ethylene substructure led to a higher entropy loss upon receptor binding, indicating that the fixed planar structure of the D-Tyr^1–L-Arg^2 peptide bond is indispensable for biological activity.

Molecular Modeling Study of Cyclic Peptidomimetics and Identification of an Alternative Binding Mode of Cyclic Pentapeptide CXCR4 Antagonists. To investigate the bioactive conformations of cyclic pentapeptide-based CXCR4 antagonists, the ^{1}H NMR spectra of **31a–d** were obtained. Peptides **31a–c** showed nuclear Overhauser effect

dx.doi.org/10.1021/jm2016914 | J. Med. Chem. 2012, 55, 2746–2757

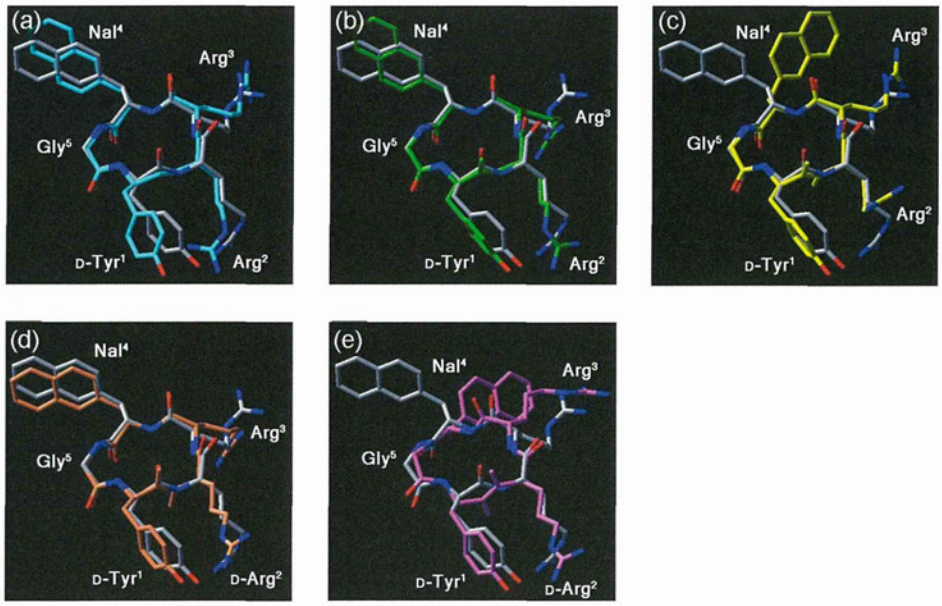

Figure 4. Superimposed low-energy structures of FC131 (gray) and the isostere-containing derivatives: (a) **31a** (blue), (b) **31b** (green), (c) **31c** (yellow), (d) **31d-A** (orange), and (e) **31d-B** (pink).

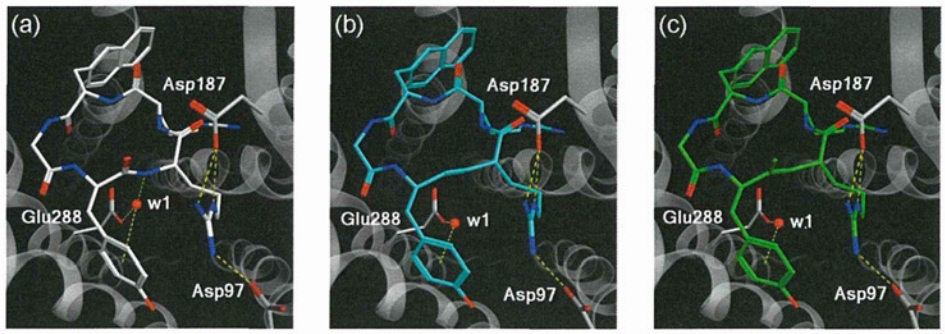

Figure 5. Binding modes of FC131 derivatives: (a) FC131, (b) **31a**, and (c) **31b**.

(NOE) patterns around the isostere similar to those seen with FC131. Interestingly, the D-Tyr[1]-D-MeArg[2] isostere-containing **31d** existed as a 1:1 mixture of two conformers; one conformer, **31d-A**, exhibited NOE patterns similar to those of FC131, and the other conformer, **31d-B**, showed different patterns. We also calculated their low-energy conformations in solution using a molecular dynamics simulation based on the NMR data. The calculations were performed by MacroModel using the Merck molecular force field (MMFFs). The backbone conformations of peptides **31a–c** and **31d-A** were similar to that of FC131 (Figure 4a–d), but **31d-B** exhibited a conformation different from that of FC131 with respect to the orientation around the isostere alkene substructure in the D-Tyr[1]-D-MeArg[2] dipeptide (Figure 4e).

Recently, we and others have reported pharmacophore models and binding models of FC131.[38–41] In our FC131–CXCR4 complex model,[41] using NMR-based calculated conformations of FC131[20,22] and an X-ray crystal structure of CXCR4[42] (Figure 5a), a guanidino group of L-Arg[2] interacts with both Asp97 and Asp187 in CXCR4, and an amide proton of L-Arg[2] forms a hydrogen bond network with Glu288 via a crystal water molecule (**w1**), which is also involved in an OH–π interaction with an aromatic ring of D-Tyr[1]. The L-Arg[3] guanidino group interacts with His113, Thr117, and Asp171 in CXCR4. In addition, the carbonyl oxygen of L-Nal[4] is involved in a second hydrogen bond network including Tyr255 and Glu288 side chains via another crystal water molecule, and hydrogen bonds are present between D-Tyr[1] phenol and Tyr45 phenol and between the carbonyl oxygen of Gly[5] and the Ser285 hydroxyl group (see the Supporting Information). Most of these interactions were maintained in all the following binding conformations of FC131 derivatives.

Using this FC131–CXCR4 complex model, we next carried out a prediction of the binding mode for **31a–d** with CXCR4. Models for binding of **31a–d** with CXCR4 were obtained by energy minimization of the complex structure using the MMFF94s force field in the Molecular Operating Environment (MOE) software package[43] (Figures 5–7). The global conformation of FC131 was little altered by substitution of the D-Tyr[1]-L-Arg[2] substructure with a disubstituted [ψ[(*E*)-CH=CH]] alkene unit in **31a** (Figure 5b). The interactions of the L-Arg[2] guanidino group and the OH–π interaction of the D-Tyr[1] phenol group with the water molecule (**w1**) were also maintained. The slightly less potent binding of **31a** may be attributable to the loss of the hydrogen bond networks by the D-Tyr[1]–L-Arg[2] peptide bond. Peptide **31b** with a ψ[(*E*)-CMe=CH] isosteric unit also exhibited a binding conformation similar to that of FC131 with the same interaction modes as those of **31a** with CXCR4 (Figure 5c). The similar biological activities and binding modes of **31a** and **31b** suggested that the

dx.doi.org/10.1021/jm2016914 | J. Med. Chem. 2012, 55, 2746–2757

steric effect of the D-Tyr[1] carbonyl oxygen in FC131 and the γ-methyl group of the isostere unit in **31b** did not cause any favorable or unfavorable interactions with CXCR4. This may be a result of the outward orientation of the D-Tyr[1] carbonyl group in FC131 from the receptor.

The whole backbone conformation of **31c** was also maintained (Figure 6b), whereas the water molecule (**w1**) was not settled below the antagonist because of the isostere β-methyl group. The lower potency of **31c** than that of **31a,b** could be rationalized by the loss of the **w1**-mediated OH−π interaction. Similarly, it was suggested that the lower receptor binding of the parent FC162 compared with that of FC131 was a result of the *N*-methyl group of L-MeArg[2] in FC162 preventing the OH−π interaction (Figure 6a).

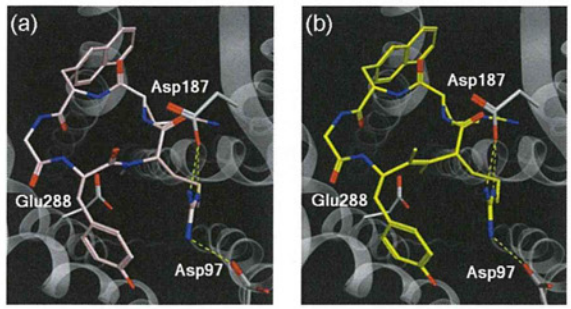

Figure 6. Binding modes of FC131 derivatives: (a) FC162 and (b) **31c**.

A calculation using the FC131-like conformer **31d-A** as an initial structure afforded a binding mode for **31d** similar to that of **31a−c**; however, the binding mode failed to provide a possible explanation for the improved bioactivity of **31d**. In contrast, an alternative reasonable binding mode of **31d** with CXCR4 was obtained when another conformation, **31d-B**, with the flipped alkene substructure was used for the calculation (Figure 7b). In this model, peptide **31d** was bound to CXCR4 at a slightly different position on CXCR4 with the **w1**-mediated OH−π interaction maintained, and the D-MeArg[2] guanidino group of **31d** bound only with Asp187 via bimodal interactions. The isostere β-methyl group may possibly restrict the peptide backbone structure to a low-energy conformation such as **31d-B**, observed in NMR analysis, which leads to decreased entropy loss upon receptor binding.

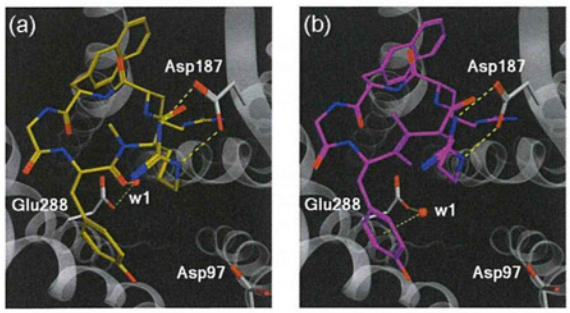

Figure 7. Binding modes of FC131 derivatives: (a) FC122 and (b) **31d**.

The binding-mode analysis of the most potent FC122 using NMR-based conformations afforded a binding structure similar to that of FC131 (data not shown); however, the highly potent activity of FC122 could not be fully rationalized by this binding mode. A possible alternative binding mode of FC122 was obtained on the basis of the characteristic binding mode of **31d**, which is the isosteric peptide corresponding to FC122 with a D-Tyr[1]-D-MeArg[2] substructure (Figure 7a). Although the binding structure of FC122 was inconsistent with its NMR-based structure with respect to the orientation of the D-Tyr[1]−D-MeArg[2] peptide bond,[41] the local conformation and binding mode around the D-Tyr[1]−D-MeArg[2] peptide bond in FC122 were similar to those of **31d**. In this binding mode, the *N*-methyl group of D-MeArg[2] in FC122 probably restricts the peptide backbone conformation, as does the isostere β-methyl group in **31d**. The less potent bioactivity of **31d** compared with that of the isosteric FC122 accounted for these similar binding modes. The D-Tyr[1] carbonyl oxygen in FC122 formed a hydrogen bond network via a water molecule (**w1**), but in **31d**, the corresponding hydrogen bond was missing because of the isosteric tetrasubstituted alkene.

In this study, docking simulations of FC131 derivatives were performed using the X-ray crystal structure of CXCR4 in a complex with a 16-residue cyclic peptide, CVX15.[42] The binding modes of FC131 and its derivatives met the requirements of the shared indispensable functional groups between CVX15 and FC131: the L-Arg[3] guanidino group and L-Nal[4] naphthalene group in FC131 correspond to Arg[2] and Nal[3] in CVX15, respectively. Although the backbone conformations varied in the cases of FC122 and **31d** as a result of the substitution mode of the D-Tyr[1]−D-MeArg[2] peptide bond, the binding modes of the side chain functional groups were maintained.

■ CONCLUSIONS

To investigate bioactive conformations, four alkene isosteres for D-Tyr[1]-L/D-Arg[2] dipeptides in the selective CXCR4 antagonist FC131 and its derivatives were synthesized. The bioactivity profiles of a series of the cyclic peptidomimetics suggested that the D-Tyr[1]−L-Arg[2] and D-Tyr[1]−L/D-MeArg[2] peptide bonds of the FC131 derivatives existed as *trans*-conformers in the bioactive conformations. In the SAR study, the tetrasubstituted alkene dipeptide isosteres adequately mimicked the *N*-methylamide bonds in D-Tyr[1]-L-MeArg[2] and D-Tyr[1]-D-MeArg[2] dipeptides. NMR studies indicated that the backbone structures of all the isostere-containing derivatives in solution were similar to that of FC131, except that a different orientation of the isostere alkene substructure was observed in **31d-B**, containing a D-Tyr[1]-D-MeArg[2] isostere. A comparative biological evaluation and binding-mode prediction suggest that the L-Arg[2] amide hydrogen in FC131 is involved in indirect receptor binding via water molecules. Although the addition of a methyl group on the D-Tyr[1]−L-Arg[2] peptide bond (FC162) or the corresponding isostere β-position (**31c**) did not influence the peptide conformation in a complex with CXCR4, the potential hydrogen bond network via water molecules in FC131 was eliminated. On the other hand, an alternative binding mode was identified in the D-MeArg[2] congener **31d**, which is the best among the isostere-containing peptides. On the basis of this binding mode of **31d**, the previously unknown binding mode of the D-MeArg[2]-substituted peptide (FC122) was identified; this was not calculated directly from the NMR-based conformations. On the basis of this binding mode for CXCR4, it is concluded that the improved potency of FC122 may be derived from a secondary conformation stabilized by both chirality and the *N*-methyl group of D-MeArg[2]. These results suggest that two distinct binding modes of cyclic pentapeptide-based

dx.doi.org/10.1021/jm2016914 | J. Med. Chem. 2012, 55, 2746−2757

CXCR4 antagonists may provide new insights into the design of more potent derivatives and small-molecule antagonists with novel scaffolds.

EXPERIMENTAL SECTION

General Procedures. All moisture-sensitive reactions were performed using syringe–septum cap techniques under an argon atmosphere, and all glassware was dried in an oven at 80 °C for 2 h prior to use. Melting points were measured by a hot stage melting point apparatus and are uncorrected. Optical rotations were measured with a JASCO P-1020 polarimeter. For flash chromatography, Wakogel C-300E was employed. For analytical HPLC, a COSMOSIL 5C18-ARII column (4.6 × 250 mm, Nacalai Tesque Inc., Kyoto, Japan) was employed with a linear gradient of MeCN containing 0.1% (v/v) TFA at a flow rate of 1 mL/min on a Shimadzu LC-20ADvp (Shimadzu Corp., Ltd., Kyoto, Japan). Preparative HPLC was performed using a COSMOSIL 5C18-ARII column (20 × 250 mm, Nacalai Tesque Inc.) with a linear gradient of MeCN containing 0.1% (v/v) TFA at a flow rate of 8 mL/min on a Shimadzu LC-6AD (Shimadzu Corp., Ltd.). ^{1}H NMR spectra were recorded using a JEOL ECA-500 spectrometer, and chemical shifts are reported in δ (ppm) relative to TMS (in $CDCl_3$) or DMSO (in DMSO-d_6) as an internal standard. ^{13}C NMR spectra were recorded using a JEOL ECA-500 spectrometer and referenced to the residual $CHCl_3$ or DMSO signal. Chemical shifts were reported in parts per million with the residual solvent peak used as an internal standard. ^{1}H NMR spectral data are given as follows: chemical shift, multiplicity (br = broad, s = singlet, d = doublet, t = triplet, q = quartet, m = multiplet), number of protons, and coupling constant(s). Exact mass (HRMS) spectra were recorded on a JMS-HX/HX 110A mass spectrometer. Infrared (IR) spectra were obtained on a JASCO FT/IR-4100 FT-IR spectrometer with a JASCO ATR PRO410-S. The purity of the peptides for bioassay was calculated as >95% by HPLC on a COSMOSIL 5C18-ARII analytical column at 220 nm absorbance (see the Supporting Information).

(3*R*,4*R*)-4-[*N*-(*tert*-Butoxycarbonyl)amino]-5-(4-methoxyphenyl)pent-1-en-3-ol (2). To a solution of LiCl (4.11 g, 96.9 mmol) and $ZnCl_2$ (13.2 g, 96.9 mmol) in THF (50 mL) was added dropwise a solution of vinylmagnesium bromide in THF (1.3 M, 75.0 mL, 96.9 mmol) at −78 °C under argon, and the mixture was stirred at 0 °C for 30 min. To a solution of Boc-L-Tyr(Me)OMe (10.0 g, 32.3 mmol) in CH_2Cl_2 (40 mL) and toluene (80 mL) was added dropwise a solution of DIBAL-H in toluene (0.99 M, 72.0 mL, 71.1 mmol) at −78 °C under argon, and the mixture was stirred at −78 °C for 30 min. To this solution was added dropwise the above solution of vinylzinc reagent at −78 °C, and the mixture was stirred for 3 h with warming to 0 °C. The reaction was quenched with 0.5 M Rochelle salt and saturated NH_4Cl. The mixture was concentrated under reduced pressure and extracted with EtOAc. The extract was washed with saturated citric acid, brine, saturated $NaHCO_3$, and brine and dried over $MgSO_4$. Concentration under reduced pressure followed by flash chromatography over silica gel with *n*-hexane–EtOAc (4:1) gave the title compound **2** (3.07 g, 9.99 mmol, 31% yield) as white solids: mp 91–92 °C; $[\alpha]_D^{28}$ +27.9 (*c* 1.39, $CHCl_3$); IR (neat) 3323 (OH and NH), 1696 (C=O); ^{1}H NMR (500 MHz, $CDCl_3$) δ 1.39 (s, 9H), 2.29–2.39 (m, 1H), 2.75–2.85 (m, 1H), 2.88 (dd, *J* = 13.7, 7.4 Hz, 1H), 3.69–3.77 (m, 1H), 3.78 (s, 3H), 4.07–4.14 (m, 1H), 4.79 (d, *J* = 6.3 Hz, 1H), 5.18 (d, *J* = 10.3 Hz, 1H), 5.27 (d, *J* = 17.2 Hz, 1H), 5.89 (ddd, *J* = 17.2, 10.3, 5.7 Hz, 1H), 6.83 (d, *J* = 8.6 Hz, 2H), 7.15 (d, *J* = 8.6 Hz, 2H); ^{13}C NMR (125 MHz, $CDCl_3$) δ 28.3 (3C), 37.0, 55.2, 56.1, 72.6, 79.4, 113.9 (2C), 116.0, 130.3 (3C), 138.4, 156.2, 158.2; HRMS (FAB) *m*/*z* calcd for $C_{17}H_{26}NO_4$ (MH^+) 308.1856, found 308.1855.

(3*R*,4*R*)-4-[*N*-(*tert*-Butoxycarbonyl)amino]-5-(4-methoxyphenyl)pent-1-en-3-yl Acetate (3). To a solution of the alcohol **2** (368.9 mg, 1.20 mmol) in $CHCl_3$ (12 mL) were added pyridine (1.94 mL, 24.0 mmol), Ac_2O (1.13 mL, 12.0 mmol), and 4-(dimethylamino)pyridine (DMAP; 14.7 mg, 0.12 mmol) at 0 °C, and the mixture was stirred for 2 h at the same temperature. The reaction was quenched with saturated NH_4Cl at 0 °C. The mixture was concentrated under reduced pressure and extracted with EtOAc. The extract was washed successively with 1 N HCl, brine, 5% $NaHCO_3$, and brine and dried over $MgSO_4$. Concentration under reduced pressure followed by flash chromatography over silica gel with *n*-hexane–EtOAc (4:1) gave the title compound **3** (418 mg, 1.20 mmol, quantitative) as colorless crystals: mp 96–97 °C; $[\alpha]_D^{26}$ +48.8 (*c* 1.21, $CHCl_3$); IR (neat) 3355 (NH), 1742 (C=O), 1712 (C=O); ^{1}H NMR (500 MHz, $CDCl_3$) δ 1.39 (s, 9H), 2.12 (s, 3H), 2.72 (d, *J* = 6.9 Hz, 2H), 3.78 (s, 3H), 3.96–4.07 (m, 1H), 4.67 (d, *J* = 9.2 Hz, 1H), 5.18–5.30 (m, 3H), 5.74–5.84 (m, 1H), 6.82 (d, *J* = 8.6 Hz, 2H), 7.08 (d, *J* = 8.6 Hz, 2H); ^{13}C NMR (125 MHz, $CDCl_3$) δ 21.0, 28.3 (3C), 37.5, 54.3, 55.2, 74.4, 79.4, 113.9 (2C), 118.0, 129.3, 130.2 (2C), 133.7, 155.4, 158.3, 169.7; HRMS (FAB) *m*/*z* calcd for $C_{19}H_{28}NO_5$ (MH^+) 350.1962, found 350.1958.

***tert*-Butyl (4*R*,5*R*,2*E*)-4-Acetoxy-5-[*N*-(*tert*-butoxycarbonyl)-amino]-6-(4-methoxyphenyl)hex-2-enoate (4).** Ozone gas was bubbled through a stirred solution of the acetate **3** (3.29 g, 9.50 mmol) in EtOAc (95 mL) at −78 °C until a blue color persisted. Me_2S (14.0 mL, 190 mmol) was added to the solution at −78 °C. After being stirred for 30 min at 0 °C, the mixture was dried over $MgSO_4$ and concentrated under reduced pressure to give the crude aldehyde, which was used for the next reaction without further purification. To a stirred suspension of LiCl (805 mg, 19.0 mmol) in MeCN (35 mL) was added *tert*-butyl diethylphosphonoacetate (4.79 g, 19.0 mmol) in MeCN (30 mL) and $(i\text{-Pr})_2$NEt (3.31 mL, 19.0 mmol) at 0 °C under argon. After 20 min, the above aldehyde in MeCN (30 mL) was added to the mixture at 0 °C, and the stirring was continued for 3 h. The reaction was quenched with saturated NH_4Cl at 0 °C. The mixture was concentrated under reduced pressure and extracted with EtOAc. The extract was washed successively with saturated citric acid, brine, 5% $NaHCO_3$, and brine and dried over $MgSO_4$. Concentration under reduced pressure followed by flash chromatography over silica gel with *n*-hexane–EtOAc (4:1) gave the title compound **4** (2.63 g, 5.85 mmol, 62% yield) as a colorless oil: $[\alpha]_D^{23}$ +44.7 (*c* 1.24, $CHCl_3$); IR (neat) 1706 (C=O); ^{1}H NMR (500 MHz, $CDCl_3$) δ 1.39 (s, 9H), 1.45 (s, 9H), 2.13 (s, 3H), 2.72 (d, *J* = 6.9 Hz, 2H), 3.77 (s, 3H), 3.97–4.15 (m, 1H), 4.50–4.70 (m, 1H), 5.38 (ddd, *J* = 5.2, 2.9, 1.1 Hz, 1H), 5.81 (dd, *J* = 15.5, 1.1 Hz, 1H), 6.69 (dd, *J* = 15.5, 5.2 Hz, 1H), 6.82 (d, *J* = 8.6 Hz, 2H), 7.06 (d, *J* = 8.6 Hz, 2H); ^{13}C NMR (125 MHz, $CDCl_3$) δ 20.3, 27.6 (3C), 27.9 (3C), 36.9, 53.7, 54.7, 72.4, 79.0, 80.1, 113.6 (2C), 124.2, 128.7, 129.7 (2C), 141.4, 154.9, 158.1, 164.4, 169.0; HRMS (FAB) *m*/*z* calcd for $C_{24}H_{34}NO_7$ (MH^-) 448.2341, found 448.2344.

***tert*-Butyl (4*R*,5*R*,2*E*)-5-[*N*-(*tert*-Butoxycarbonyl)amino]-4-hydroxy-6-(4-methoxyphenyl)hex-2-enoate (5).** To a solution of the acetate **4** (1.21 g, 2.70 mmol) in MeOH (27 mL) was added K_2CO_3 (746 mg, 5.40 mmol) at 0 °C, and the mixture was stirred for 2 h at room temperature. After the mixture was filtered, the filtrate was concentrated under reduced pressure and extracted with EtOAc. The extract was washed with brine and dried over $MgSO_4$. Concentration under reduced pressure followed by flash chromatography over silica gel with *n*-hexane–EtOAc (3:1) gave the title compound **5** (1.06 g, 2.60 mmol, 96% yield) as colorless solids: mp 98–99 °C; $[\alpha]_D^{24}$ +60.3 (*c* 1.04, $CHCl_3$); IR (neat) 3436 (OH and NH), 1698 (C=O); ^{1}H NMR (500 MHz, $CDCl_3$) δ 1.38 (s, 9H), 1.45 (s, 9H), 2.81 (dd, *J* = 13.7, 7.4 Hz, 1H), 2.90 (dd, *J* = 13.7, 7.4 Hz, 1H), 3.75 (s, 3H), 3.77–3.85 (m, 1H), 4.23–4.27 (m, 1H), 4.96–5.05 (m, 1H), 5.98 (dd, *J* = 15.5, 1.7 Hz, 1H), 6.78–6.84 (m, 3H), 7.14 (d, *J* = 8.6 Hz, 2H); ^{13}C NMR (125 MHz, $CDCl_3$) δ 28.0 (3C), 28.2 (3C), 36.8, 55.06, 55.09, 70.8, 79.5, 80.3, 114.0 (2C), 123.3, 130.07 (2C), 130.10, 146.8, 156.0, 158.3, 165.6. Anal. Calcd for $C_{22}H_{33}NO_6$: C, 64.84; H, 8.16; N, 3.44. Found: C, 64.67; H, 8.19; N, 3.55.

***tert*-Butyl (4*R*,5*R*,2*E*)-5-[*N*-(*tert*-Butoxycarbonyl)amino]-4-[(methylsulfonyl)oxy]-6-(4-methoxyphenyl)hex-2-enoate (6).** To a stirred solution of the alcohol **5** (897 mg, 2.20 mmol) in CH_2Cl_2 (22 mL) were added Et_3N (3.06 mL, 22.0 mmol) and methanesulfonyl chloride (851 μL, 11.0 mmol) at 0 °C, and the mixture was stirred for 2 h at the same temperature. After the reaction was quenched with water, the mixture was concentrated under reduced pressure, and the residue was extracted with EtOAc. The extract was